Contract AF33(615)-1150

Final Report

SPECTROSCOPIC STUDIES OF THE VAPORIZATION OF REFRACTORY MATERIALS

November 1964

SPACE SCIENCES LABORATORY

MISSILE AND SPACE DIVISION

GENERAL ELECTRIC

SPECTROSCOPIC STUDIES OF THE VAPORIZATION OF REFRACTORY MATERIALS

Final Report

ARPA Order No. 24

Amendment No. 72, Task 6

Project No. 4776

Program Code No. 4910

Contract Number:	AF 33(615)-1150
Date of Contract:	1 November 1963
Date Contract Expires:	30 November 1964

Project Scientist

Dr. Milton J. Linevsky

Telephone Area Code 215-969-3495

November 30, 1964

Space Sciences Laboratory
General Electric Company
Box 8555, Philadelphia 1, Penna.

TABLE OF CONTENTS

LIST OF FIGURES

LIST OF TABLES

ABSTRACT

The technique of matrix isolation has been used to obtain the infrared spectra of several high temperature molecules. A double boiler and reaction oven type Knudsen cell technique have been added to the general methods of matrix isolation resulting in greater versatility of the method. Differentiation between monomer and polymer spectra appears to be entirely possible.

The following molecules have been studied: MgF_2, AlF_3, Li_2F_2, ThO_2, ThO, ZrO_2 and ZrO. In most cases tentative frequency assignments have been made and structural properties inferred.

Atomic resonance line absorption studies have been carried out on HfB_2, TiN and ZrN. Heats of formation have been obtained based on the observed vapor pressures.

I. INTRODUCTION

The material reported herein, represents a one year effort into (1) the study of the spectroscopic properties, principally the infrared spectra, of several substances which are important either as combustion products of possible rocket fuels or as high temperature refractory materials and (2) the use of spectroscopic techniques to measure the vapor pressure of atomic species over several refractory substances. This work essentially is a continuation of part of a program originally initiated in November of 1959 which was undertaken to provide data, design information, and selection criteria for materials suitable for uncooled rocket nozzle fabrication.

This report presents details of the work and the results obtained during the period 1 November 1963 through 30 November 1964. No effort has been made to include the results of earlier studies, reported in prior annual reports (References 1, 2, 3, and 4).

As indicated above, this program consists of two separate areas of investigation: 1) Matrix isolation studies -- to obtain information about the spectra and structure of

high temperature molecules and 2) resonance line absorption studies -- to directly measure the vapor pressure of atomic species in equilibrium with refractory substances by optical spectroscopic techniques.

II. MATRIX ISOLATION STUDIES

A. Background and Introduction

The application of the matrix isolation technique to high temperature vapors[5] has provided a new source of experimental spectroscopic data which heretofore was unattainable. The technique has proved itself particularly well suited to the study of the infrared spectra of high temperature molecular species, and when used with isotopically enriched materials has provided a powerful means of elucidating molecular structure[6,7,8]. It is probably the only technique capable of yielding structural information on high temperature polyatomic molecules albeit this data is admittedly approximate.

The molecules which have received attention during this report period fall into two categories: 1) several light metal fluorides important as possible rocket fuel combustion products. The molecules studied in this group

are MgF_2, AlF_3, LiF and AlOF; 2) The very refractory heavy metal oxides, ThO_2 and ZrO_2. This group represents an extension of previous work which has been reported in several annual reports[2,3,4].

During the past year, several modifications of the basic matrix isolation method have been made. Perhaps the most significant of which has been the introduction of a double oven technique which has proved to be quite successful in differentiating between polymer and monomer species. It is based on the fact that if the saturated vapor containing both monomer and polymer molecules above a condensed phase is super-heated in the absence of the condensed phase, the equilibrium established is such that the monomeric species are greatly enhanced in concentration depending upon the heat of polymerization. Although this technique is not new and has been successfully used in mass spectrometric studies involving Knudsen effusion, it represents a new innovation with the use of the matrix isolation method for high temperature materials. In the cases of AlF_3 and LiF the use of the technique allows an unambiguous assignment of monomer and polymer bands, however, in the case of MgF_2, the results

appear inconclusive insofar as differentiating between monomer and polymer. Details of the double oven will be presented in a later section. This double oven innovation was not attempted on the very refractory oxides ThO_2 and ZrO_2 because of the severe temperatures that would be necessary to maintain effective double oven conditions.

A second innovation introduced during the past year has been that of a reaction type Knudsen cell. In this method a hot vapor is generated in one part of a Knudsen cell and is then allowed to react with a second condensed phase at a higher temperature in a different part of the cell. The resulting vapor is then matrix isolated in the conventional manner. Use of this technique was attempted in the AlOF study and although the results were negative, the innovation appears to be a useful adjutant to the matrix isolation technique and therefore, its description has been included here.

B. Experimental

The basic experimental techniques have been adequately described elsewhere[5]. As mentioned above a double oven innovation has been added to the technique. The double oven

simply replaces the usual single boiler Knudsen cell in the experimental arrangement. A simple double boiler Knudsen cell was constructed of molybdenum and is depicted in Figure 1. The length of the top boiler (dimension "A"), to a large extent, determines the temperature difference which can be achieved between top and bottom boilers; also the position of the cell relative to the center of the induction coils has a significant effect on this temperature difference. We have been able to obtain temperature differences ranging from 200°C to 700°C by a judicious choice of dimensions and placement.

The long wavelength capability of our instrumentation has also been extended to around 55.5 microns (180 cm^{-1}). This has been accomplished through the modification of the model 12 grating instrument by replacing the grating with one blazed for the 45 μ region and by using various filters and restrallen plate combinations.

Magnesium Fluoride - Matrix isolation of the vapors generated from a sample of spectroscopic grade MgF_2 was carried out in both argon and krypton matrices. Vaporization from both single boiler platinum cells and double boiler

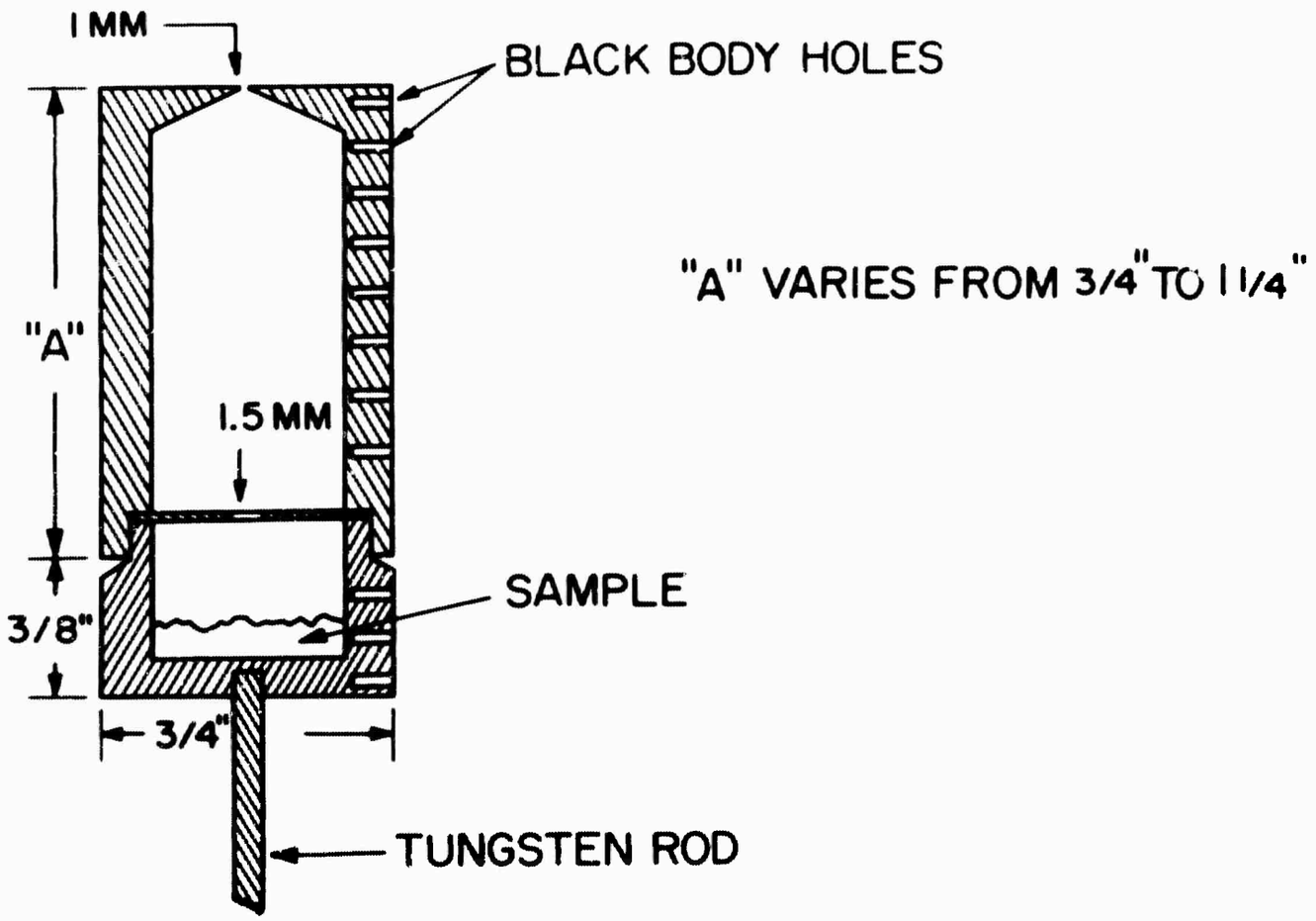

Figure 1. Double Boiler Knudsen Cell

molybdenum cells was performed at temperatures varying from 1225°C to 1380°C. There was no apparent effect on the spectra due to the different metallic nature of the Knudsen cells used in the vaporization. The single boiler results appear in Figure 2 while the double boiler results are given in Figure 3. It should be noted that the long wavelength spectrum given in Figure 3 was obtained by using the grating instrumentation and that the band previously seen at 247 cm^{-1} (Figure 2) is resolved into several features as seen in Figure 3.

Aluminum Trifluoride - A sample of high purity anhydrous AlF_3 was obtained through the courtesy of the Kaiser Aluminum Corporation; this material had a purity of better than 99%. Isolation was carried out in argon, krypton and xenon matrices using both a single boiler platinum cell and a double boiler molybdenum cell. Here again no apparent effect on the spectra, due to the different metallic nature of the Knudsen cells, was evident. Typical results and conditions of isolation are given in Figures 4 and 5.

Aluminum Oxy-Fluoride - AlOF - Several attempts were made to obtain the matrix isolated spectrum of AlOF using

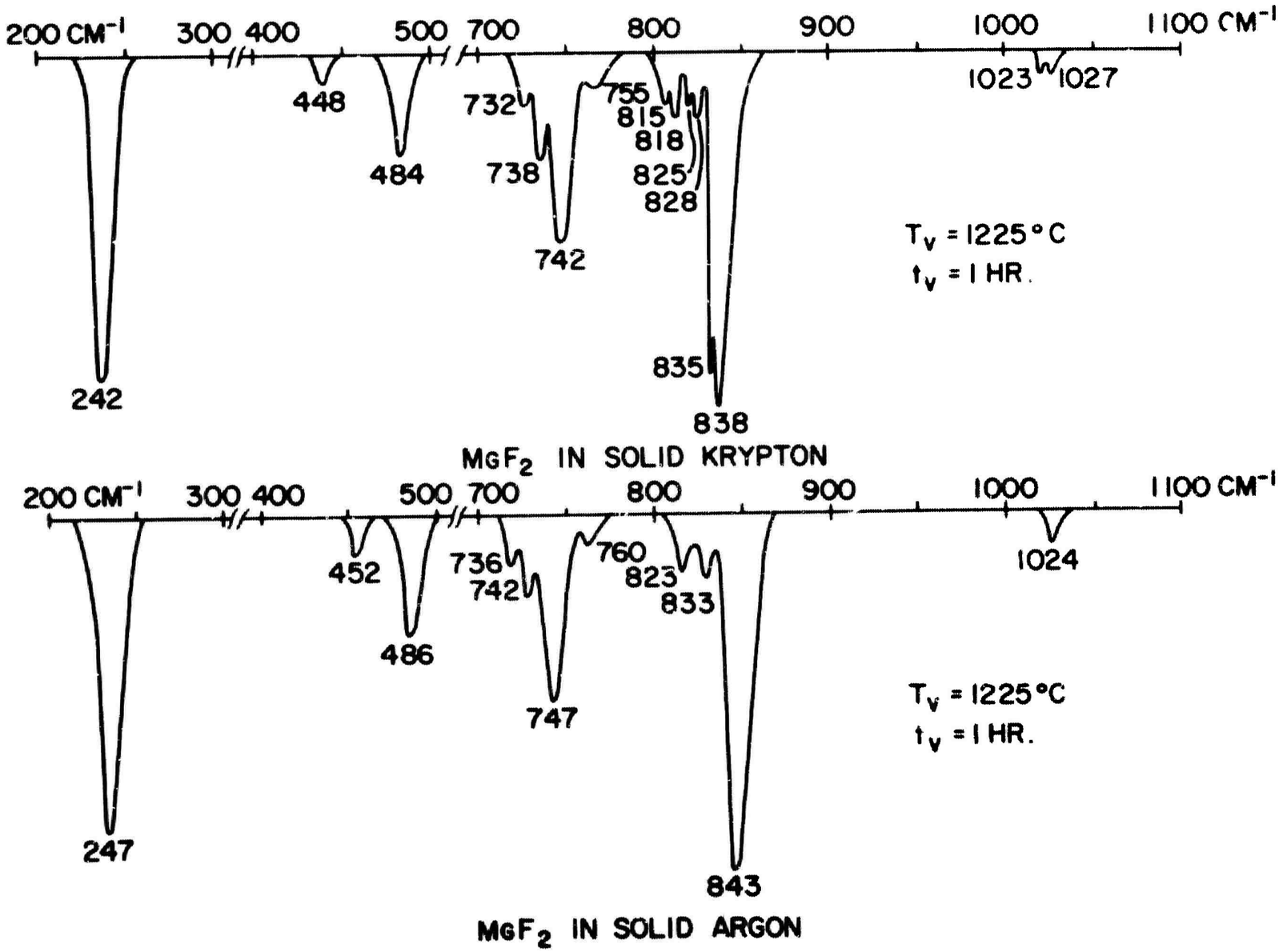

Figure 2. Infrared Spectrum of MgF_2

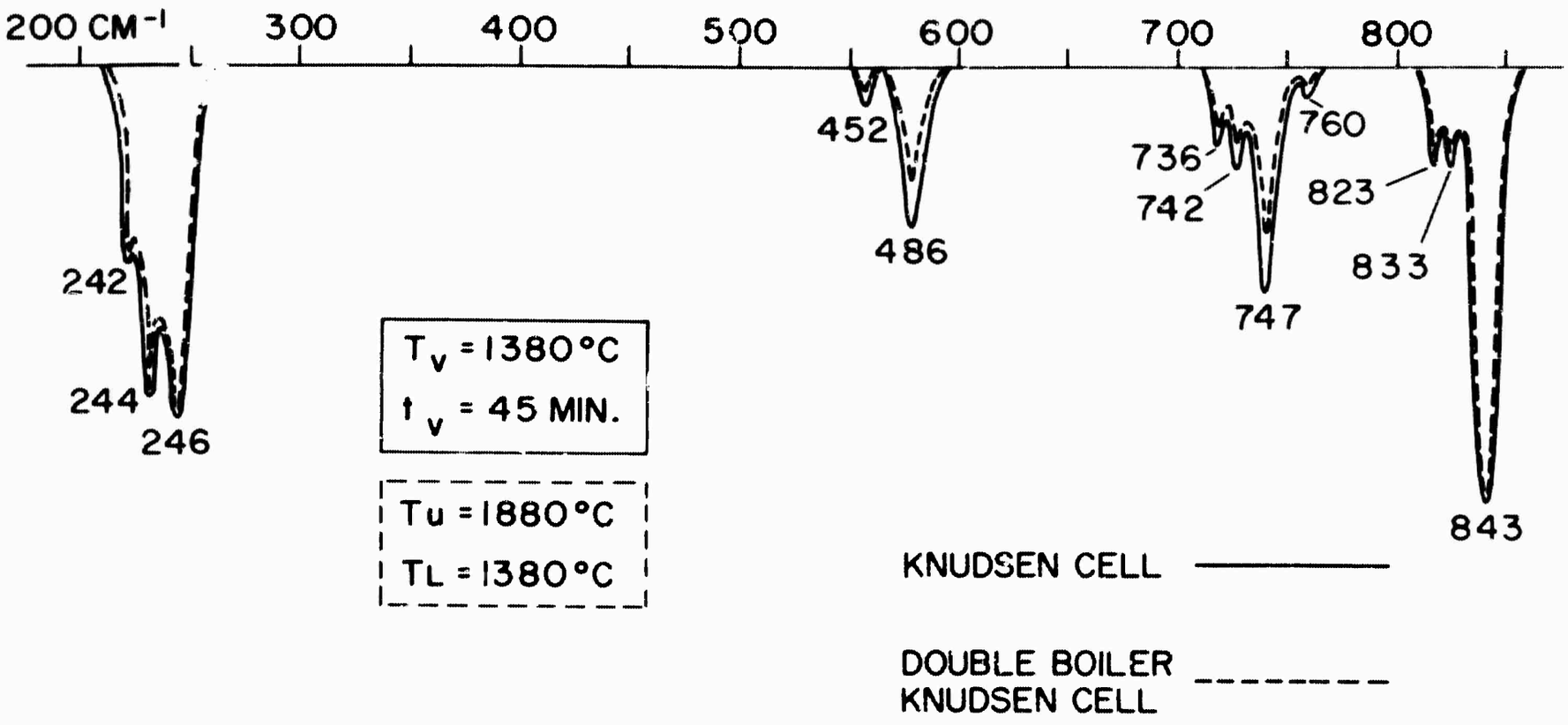

Figure 3. The Infrared Spectrum of MgF_2 in Solid Argon - Double Boiler

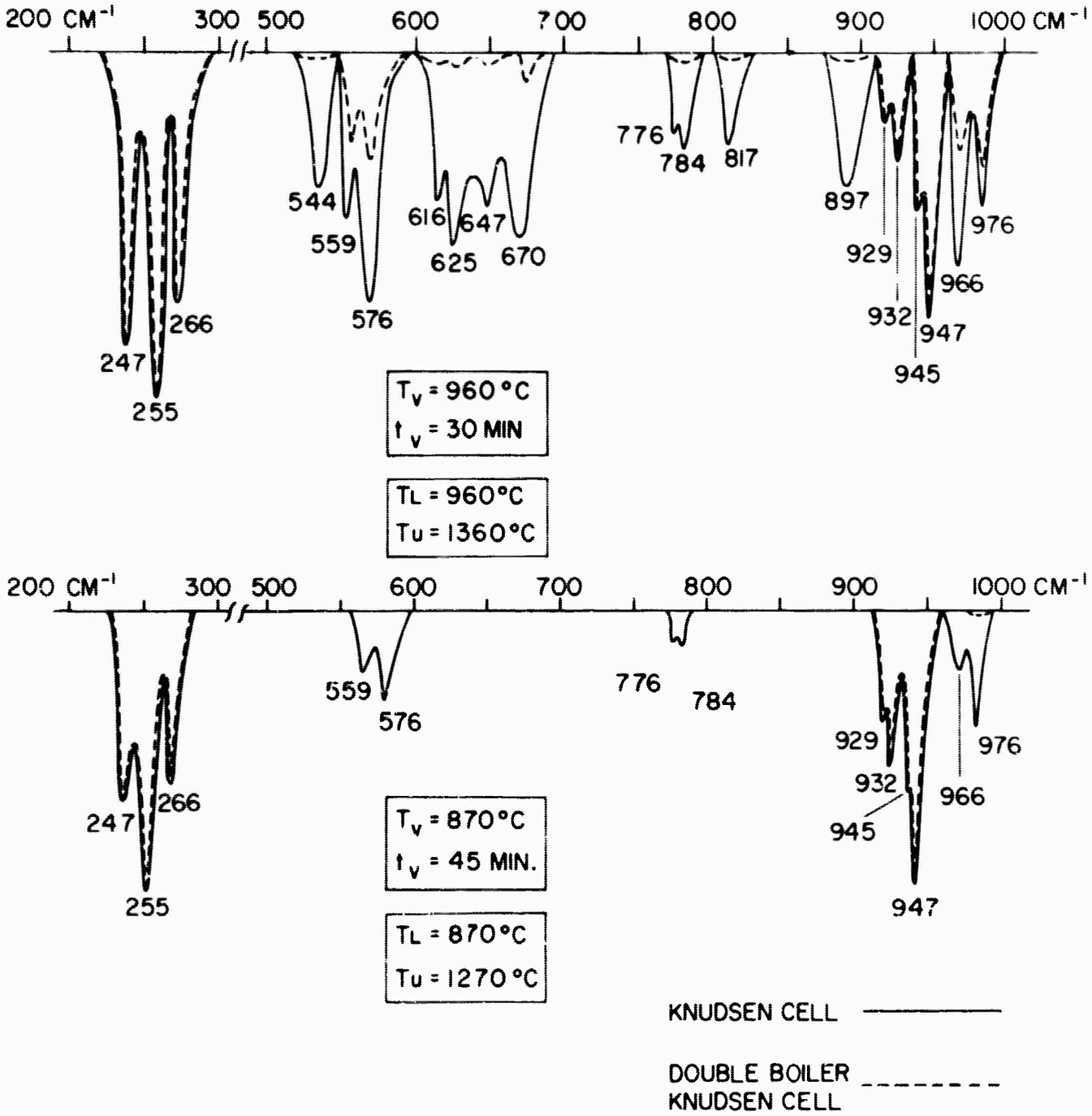

Figure 4. AlF_3 in Solid Argon

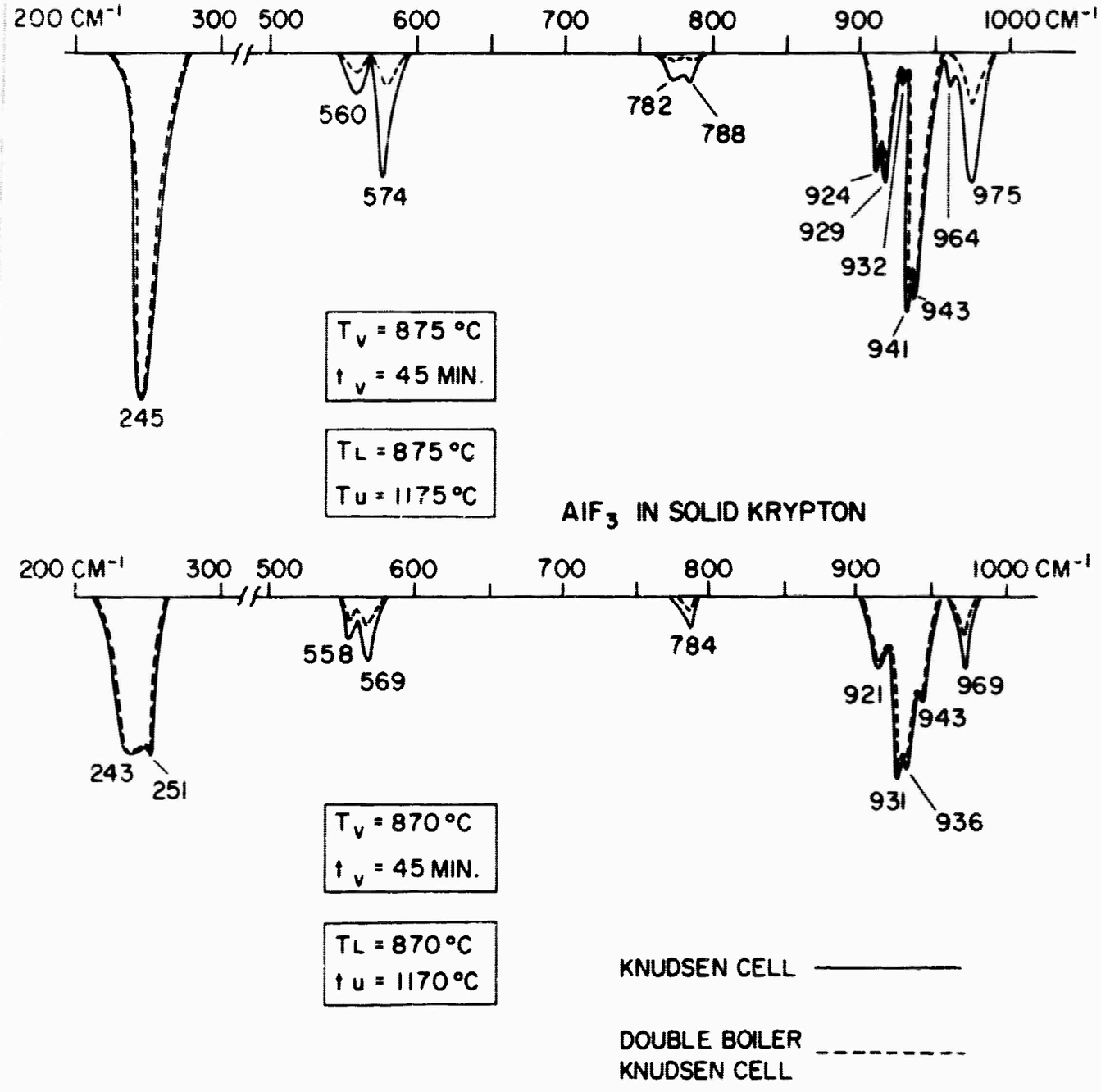

Figure 5. AlF_3 in Solid Xenon

the previously mentioned reaction Knudsen cell. Essentially this cell is simply a modification of the double oven type cell except that prior to leaving the cell the hot vapor is allowed to come in contact with a second condensed phase so that a reaction between the two can take place. A typical cell is shown schematically in Figure 6. In the case of AlOF, AlF_3 was placed in the bottom container of the cell and was vaporized at 950°C. These vapors were then super-heated to around 1900°C and were allowed to perculate through hot alumina in hopes of generating AlOF by the following reaction

$$AlF_3(g) + Al_2O_3(s) = 3\ AlOF(g) \qquad (1)$$

Although the only spectrum obtained was that of AlF_3, the technique appeared worthwhile as an adjunct to the matrix isolation of hot vapors and for this reason, its description has been included here.

Lithium Fluoride - The infrared spectrum of matrix isolated lithium fluoride has been reported before[9]. However, with the introduction of the double oven technique and with the added wavelength coverage of our grating instrumentation, it was decided to reexamine the spectrum of this material. A 50-50 mixture of the isotopic species Li^6F and Li^7F was

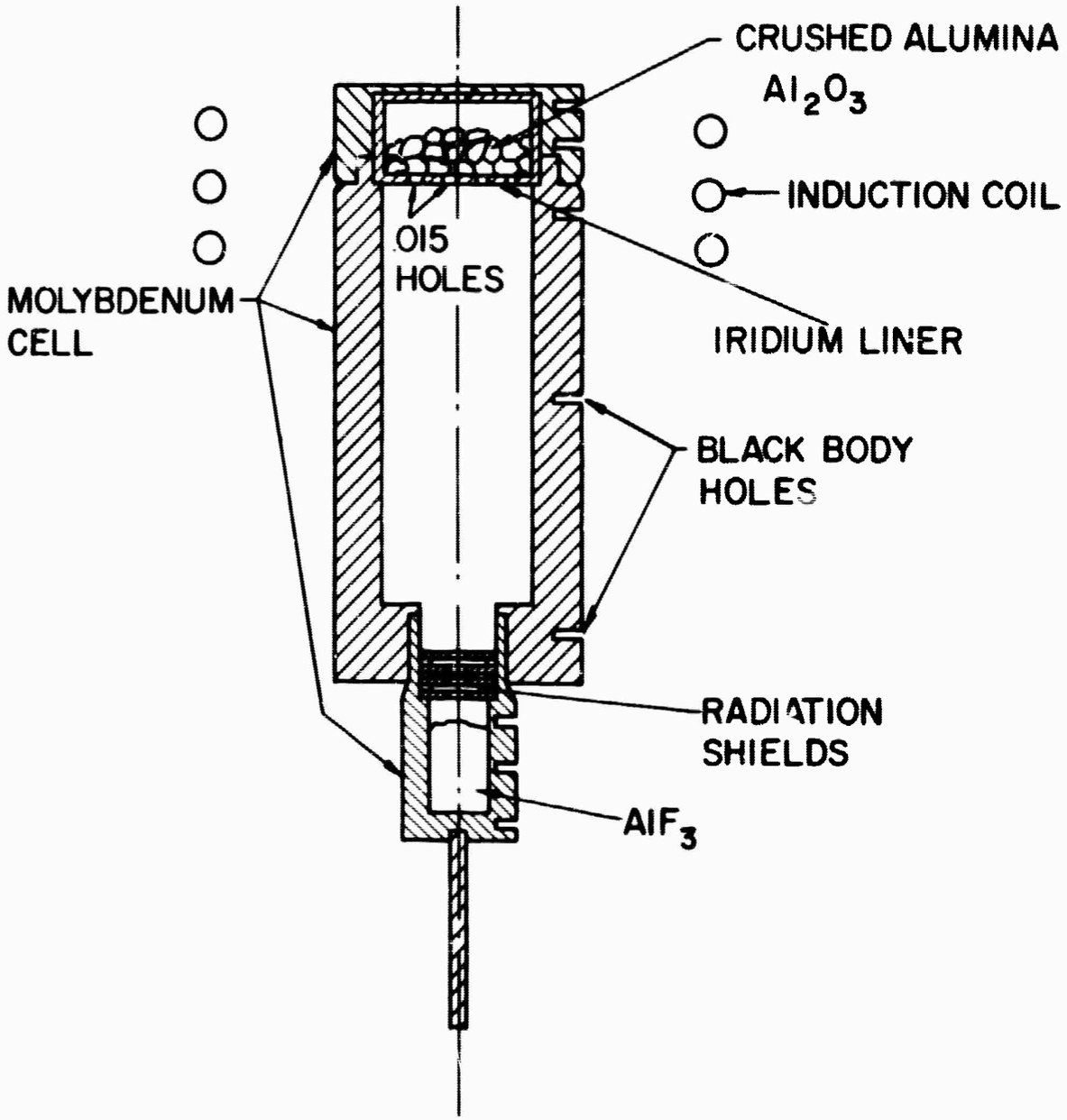

Figure 6. Reaction Knudsen Cell

vaporized from a platinum cell in the conventional manner and also from a double oven Knudsen cell. The spectra were obtained in solid argon and are shown in Figure 7.

Thoria - The matrix isolated spectrum of the vapor species in equilibrium with thoria has been given in several previous reports[3,4]. During the past year the spectrum was reexamined using isotopically enriched materials. A sample of O^{18} enriched ThO_2 was obtained from the Volk Radio-Chemical Company. The enrichment being approximately 45%. The material was loaded into a standard tungsten Knudsen cell and was degassed in the usual fashion. Degassing of the sample proved to be a long and arduous task since the material was contaminated with a large amount of ammonium chloride resulting from the preparative process. The spectrum of this isotopically enriched sample was obtained in solid argon in the region 2 μ to 55.5 μ and a typical spectrum and conditions are given in Figure 8.

Zirconia - The matrix isolated spectrum of the vapor species in equilibrium with zirconia has also been given in previous reports[3,4]. Here again the spectra were reexamined using isotopically enriched materials. However, in this

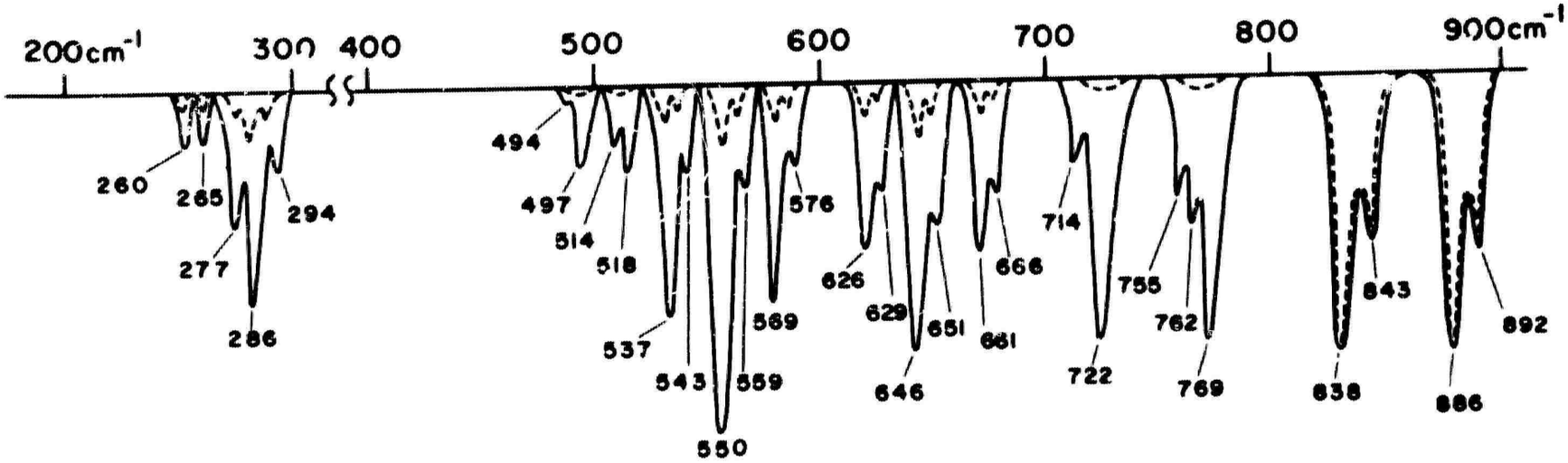

SINGLE BOILER KNUDSEN CELL ———
T_v = 930°C t_v = 1 hr

DOUBLE BOILER KNUDSEN CELL – – –
T_v = 930°C - 1230°C t_v = 1 hr

Figure 7. $Li^{6-7}F$ in Solid Argon

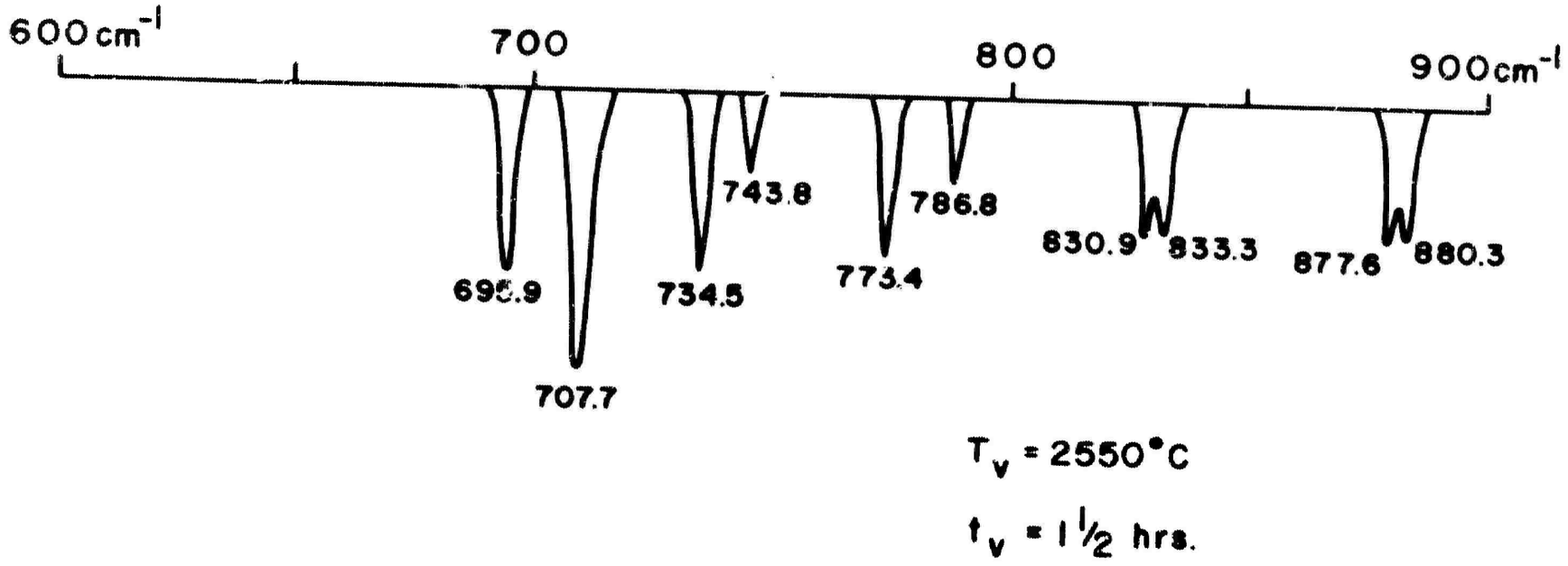

Figure 8. Infrared Spectrum of ThO_2^{16} - ThO_2^{18} in Solid Argon

case since the zirconium isotopes were also readily available, spectra were obtained not only on O^{18} enriched ZrO_2 but also on the Zr^{90} and Zr^{94} enriched materials. A sample of approximated 35% O^{18} enriched ZrO_2 was obtained from the Volk Radio-Chemical Company whereas samples of approximately 96% enrichment of Zr^{90} and Zr^{94} were obtained from the Oak Ridge National Laboratories. The 35% O^{18} enriched material was vaporized in manner completely analogous to the thoria work. In the case of the isotopically enriched zirconium material, a 50-50 mixture of the Zr^{90} and Zr^{94} material was used. Typical spectra and conditions are given in Figure 9. It should be noted that this latter spectrum was obtained using the grating instrumentation and therefore, there are small discrepancies between the values of the frequencies obtained here as compared with the corresponding frequencies appearing in the other spectra. It is felt that the grating frequencies are more accurate and that indeed where small changes due to isotopic substitution (such as Zr^{90} and Zr^{94}) are found, these frequencies are to be preferred.

C. Results and Discussion

Magnesium Fluoride - If MgF_2 is linear then the infrared

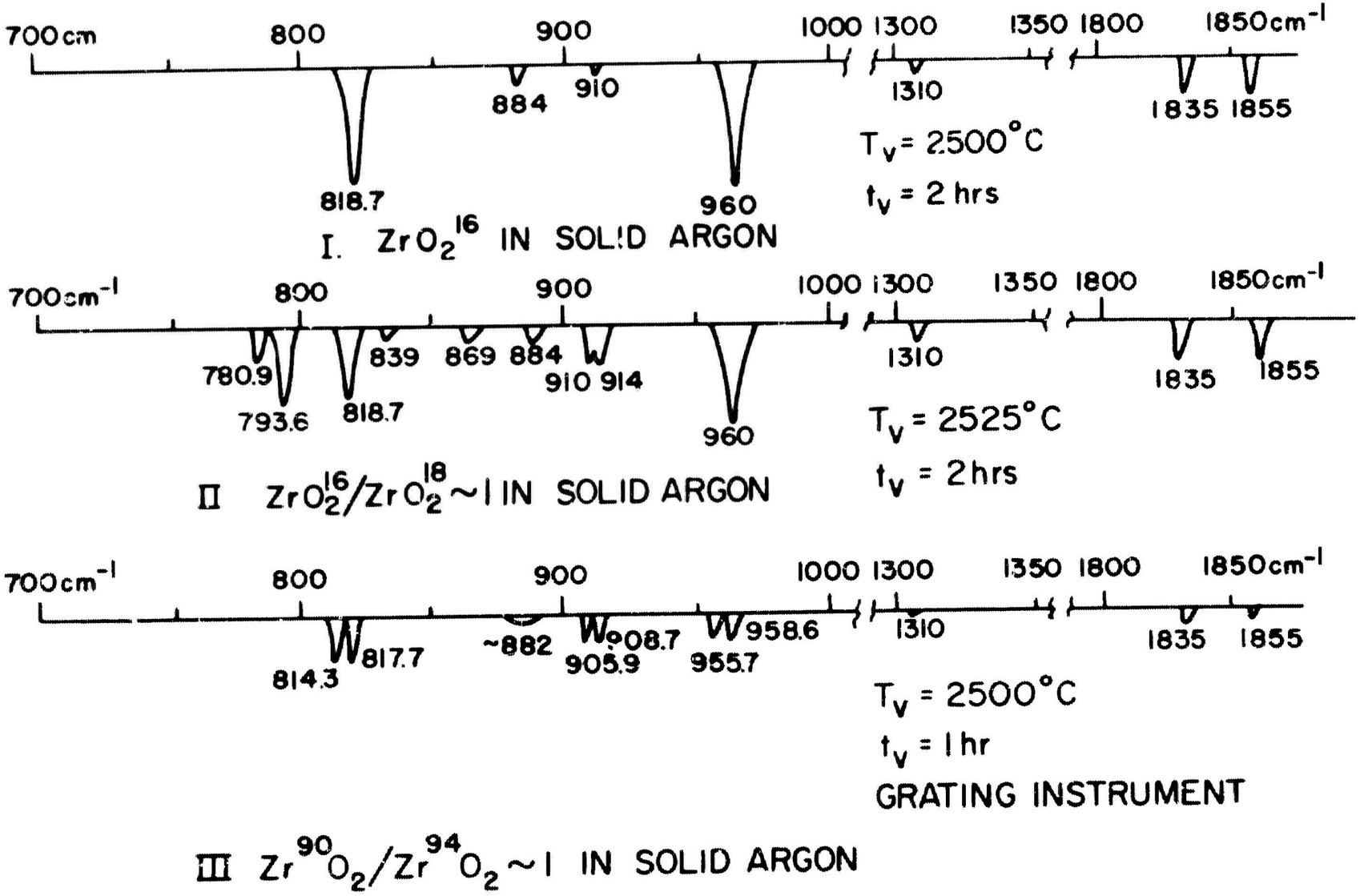

Figure 9. Infrared Spectrum of Zirconia

spectrum should consist of two fundamental frequencies, ν_3, the asymmetric stretch and ν_2, the bending mode. On the other hand, if the molecule is bent, the symmetric stretching mode ν_1 should also be active. There is little doubt that the frequencies occuring in the 800 cm^{-1} to 900 cm^{-1} region depicted in Figures 2 and 3 are to be assigned to ν_3. Since magnesium has three naturally occuring isotopes (Mg^{24} - 78.6%, Mg^{25} - 10.1% and Mg^{26} - 11.3%), the following isotopic species should be evident in the spectrum: $Mg^{24}F_2$, $Mg^{25}F_2$ and $Mg^{26}F_2$ and should occur in the intensity ratios of their isotopic abundances. Indeed the features around 800 cm^{-1} show this triplet behavior. An indication of the F Mg F angle can be obtained from the isotopic shifts of these bands and leads to an angle of $160^{\circ} \pm 20^{\circ}$. It is therefore, difficult to conclude whether or not ν_1 the symmetric stretching mode will be sufficiently active to be seen. On first examination of Figure 2 it might be concluded that one of the features in the 500 cm^{-1} to 700 cm^{-1} region could be assigned to ν_1. However, although not entirely conclusive, the double boiler results given in Figure 3 indicate that these bands are possibly due to polymeric

species. It was also noted, in several single boiler experiments, that the ratio of the relative intensities of these bands to the major band at 843 cm^{-1} (in argon) appeared to vary with the temperature of the vaporizing material which may indicate that indeed these bands belong to different molecular species than do the 843 cm^{-1} bands. Furthermore, in the case of the bands at 843 cm^{-1}, 833 cm^{-1} and 823 cm^{-1} (in argon) which have been assigned to ν_3 of the species $Mg^{24}F_2$, $Mg^{25}F_2$ and $Mg^{26}F_2$, respectively, the relative intensities (log I/I_o) of these bands agree quite well with the isotopic abundances of the magnesium isotopes, namely 79%, 10% and 11%. However, in the case of the bands at 747 cm^{-1}, 742 cm^{-1} and 736 cm^{-1} (in argon) the agreement between the relative intensities and abundances is not good. Indeed good agreement is obtained if it is assumed that these frequencies belong to the dimer species $Mg_2{}^{24}F_4$, $Mg^{24}Mg^{25}F_4$ and $Mg^{24}Mg^{26}F_4$, respectively. In this case, the natural abundances are approximately 62%, 16% and 18% respectively.

In the long wavelength region of the spectrum it is seen from Figures 2 and 3 that depending upon the instrumentation

used, one or more features are observed around 250 cm^{-1}. The frequency at 247 cm^{-1} (in solid argon) appears as a triplet when reexamined with the grating instrumentation (Figure 3). The separation between peaks is approximately 2 cm^{-1}. Indeed a bending frequency, ν_2, in this region is to be expected having a triplet structure due to three different isotopic molecules. The isotopic separation of this triplet (2 cm^{-1}) further confirms the bent nature of MgF_2 since if this molecule were linear a predicted value of 3 cm^{-1} should be observed; any smaller value indicates a non-linear configuration. It would then appear that ν_2, the symmetric bending frequency, has been observed, however, the apparent relative intensities of the observed frequencies as seen in Figure 3, are somewhat inconsistent with the isotopic distribution and for this reason this assignment of ν_2 to the observed long wavelength triplet should be taken as tentative. The complete resolution of this problem must await the use of pure isotopically enriched materials.

In conclusion, the assignment of ν_3 appears to be quite certain and that of ν_2 although not as certain, at least can be made tentatively from the observed spectrum.

The situation with ν_1 unfortunately is much more dubious since there is some evidence that bands which could be assigned to this mode are indeed due to polymeric species. The negative observation of ν_1 would imply that the molecule is linear or nearly so -- this result would not be inconsistent with the observed spectrum since the calculated angle appears to be rather large. Nevertheless, a frequency for ν_1 should be expected around 500 cm^{-1} and indeed using this value along with the observed values for ν_2 and ν_3, the agreement between the calculated and observed free energy functions for MgF_2 is greatly improved over the previous estimates. This is illustrated in Table I where the calculated fef based on the old linear models[10,11] and the assignment as given here are compared with the observed second law free energy functions.

Aluminum Trifluoride - From an examination of Figures 4 and 5, it is quite evident that the saturated vapor in equilibrium with AlF_3 contains appreciable amounts of polymeric species. Indeed the attenuation of these polymers is quite dramatic when the double boiler results are compared with the single boiler Knudsen cell spectra. There

TABLE I

COMPARISON OF EXPERIMENTAL AND ESTIMATED

VALUES OF $-(F^{o}-H^{o}_{298})/T$ FOR $MgF_2(g)$

Temperature °K	$-(F-H^{o}_{298})/T$ cal/deg/mole		
	Second Law	Third Law[a]	Third Law[b]
1500	69.8	66.3	68.9
2000	73.8	69.7	72.1

a. Previous linear model $\nu_1 = 535$, $\nu_2 = 479$, $\nu_3 = 858$

b. Bent model F Mg F = 160° $\nu_1 \sim 500$, $\nu_2 = 247$, $\nu_3 = 843$

is little question as to which spectral features are due to monomeric species.

Presumably AlF_3 has a plane symmetrical structure (D_{3h}) as do the boron trihalides. For this symmetry, there are three infrared active vibrations. Two of these consist primarily of angle bending motions and should occur at relatively low frequencies. The other one, involving a stretching motion, should occur at a much higher frequency. Indeed examination of Figures 4 and 5, especially the argon results, show three groups of bands which are not attenuated by the double boiler. In the case of krypton only, a single low frequency is evident. However, since the observed band (245 cm^{-1}) is unusually broad, there indeed may be two bands present. Using BF_3 as a guide[12], a tentative assignment has been carried out for the observed monomer frequencies. These results are given in Table II.

It is interesting to note that, in the case of the frequencies assigned to the doubly degenerate E' modes (ν_3 and ν_4), there appears to be a removal of the double degeneracy by the matrix, especially by argon. The high frequency mode, ν_3, appears as two features around 949 cm^{-1}

TABLE II

TENTATIVE VIBRATIONAL FREQUENCY

ASSIGNMENT FOR $AlF_3(g)$

Frequency Argon cm^{-1}	Frequency Krypton cm^{-1}	Frequency Xenon cm^{-1}	Assignment	Remarks
947	943	943		ν_1 (A'_1)
945	941	936		Estimated
		931	ν_3 (E')	= 646 cm^{-1}
932	929			K_1 = 4.67 md/A
929	924	921		$\frac{K\delta}{\ell^2}$ = .48 md/A
266		251	ν_2 (A''_2)	$\frac{K\Delta}{\ell^2}$ = .25 md/A
255	245	243	ν_4 (E')	
247				

and 932 cm^{-1} and the low frequency mode, ν_4, also appears as two features at 255 cm^{-1} and 243 cm^{-1}. Such behavior is really not unexpected since it is quite plausible that matrix interactions with a degenerate vibration can result in the removal of the degeneracy.

Using a three term quadratic potential for a planar XY_3 molecule, as given in Herzberg[12], and the observed frequencies in argon $\left[\nu_2(A_2') = 266\ cm^{-1},\ \nu_3(E')\right.$ approximately 940 cm^{-1}, and $\left.\nu_4(E')$ approximately 251 $cm^{-1}\right]$, the inactive unobserved frequency $\nu_1(A_1')$ and the vibrational force constants can be calculated. These results are presented below:

$$\nu_1(A_1') = 646\ cm^{-1}$$

$$K_1 = 4.67\ md/A.$$

$$\frac{K\delta}{l^2} = .48\ md/A.$$

$$\frac{K\Delta}{l^2} = .25\ md/A.$$

No attempt to analyze the polymer spectrum has been made as yet.

Aluminum Oxy-Fluoride - AlOF - As mentioned in the previous section, the only spectrum obtained in this study

was that of AlF_3. This result is somewhat surprising since presumably AlOF has been generated in the same manner described by Farber and Peterson[13]. These authors based their conclusions on a weight loss method and may indeed be misleading since no specific observation (such as the mass spectrum) of the AlOF molecule was made. Further study of this problem is indicated.

Lithium Fluoride - An examination of Figure 7 reveals the rather dramatic attenuation of the polymeric bands by the double oven technique. There is little doubt that all the spectral features below 838 cm^{-1} must be due to polymer molecules. Indeed in a recent paper[9] where the spectrum was obtained only to 300 cm^{-1}, the two strong triplets (537, 550, 569 and 626, 646 and 661) were assigned to the B_{2u} and B_{3u} modes of a planar rhomboid dimer, Li_2F_2. At that time the other expected infrared active frequency, the B_{1u} mode was not observed and was presumed to be below the range of our measurements. With the extended instrumentation used in this study, a reexamination of a 50-50 mixture of Li^7F and Li^6F (Figure 7) indeed shows the presence of the third triplet at 294 cm^{-1}, 286 cm^{-1} and 277 cm^{-1}. The isotope

frequency ratio agrees exactly, within experimental error, with the predicted ratio for the B_{1u} mode. It is also quite evident from Figure 7 that these frequencies are greatly attenuated by the double oven indicating polymeric species.

The two doublets at 497 cm^{-1}, 518 cm^{-1} and 722 cm^{-1}, 769 cm^{-1} were originally thought to be due to matrix effects. However, with the observation of a third doublet at 260 cm^{-1}, 265 cm^{-1}, this explanation appears to be improbable. It has been suggested that these spectral features are due to the formation of LiF_2^- in the matrix. On the basis of this rather speculative assumption an assignment of the doublet at 722 cm^{-1}, 769 cm^{-1} to ν_3, the doublet at 497 cm^{-1}, 518 cm^{-1} to ν_1 and the doublet at 260 cm^{-1}, 265 cm^{-1} to ν_2 of the isotopic molecules $Li^7F_2^-$ and $Li^6F_2^-$ respectively appears to be quite possible. This assignment implies that the molecule LiF_2^- is bent and indeed the apex angle is calculated to be around 120°. This result is inconsistent with the present ideas of molecular bonding since a molecule like LiF_2^-, being isoelectronic with CO_2 should be linear. However, it is entirely possible that the LiF_2^- molecule is highly distorted by the presence of the Li^+ and that both species remain

trapped in a matrix site and exist as a complex such as:

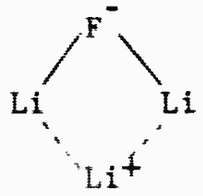

These thoughts should be taken as highly speculative, however, they serve to rather nicely explain the observed spectrum.

Thoria - In a previous annual report, the infrared spectrum of ThO_2^{16} was given[4]. From a comparison of Figure 8 with the O^{16} spectrum, the identification of those features belonging to the various isotopic molecular species is obvious. The spectrum consists of two triplets and a doublet; the triplets being due to the ThO_2 species ThO_2^{16}, $ThO^{16}O^{18}$, and ThO_2^{18} while the doublet is due to the ThO species ThO^{16} and ThO^{18}. The relative intensities of observed features are consistent with the isotopic enrichment of the sample. The triplet, 734.5 cm^{-1}, 707.7 cm^{-1} and 695.9 cm^{-1}, due to the species ThO_2^{16}, $ThO^{16}O^{18}$ and ThO_2^{18}, respectively constitutes the most intense feature of the observed spectrum and must be assigned to ν_3 the asymmetric stretch. From the values 734.5 cm^{-1} and 695.9 cm^{-1} an estimate of the

apex angle can be made. This results in a value for the apex angle around 106°. It should be pointed out that because of the massiveness of the central thorium atom in ThO_2, the calculation of the apex angle from the isotopic frequencies is not very sensitive. Nevertheless, it is felt that this result indicates strongly that the ThO_2 molecule is highiy bent. In view of this result, it becomes quite plausible to assign the other triplet (786.8 cm^{-1}, 773.4 cm^{-1} and 743.8 cm^{-1}) to ν_1 the symmetric stretching mode. Since for molecules which are highiy bent it is not unusual to have ν_1 occur at higher frequencies than ν_3[14]. The doublet, 877.6 - 880.3 cm^{-1} and 830.9 and 833.3 cm^{-1}, the higher member of which was previously proven to be due to ThO^{16}, yields an isotope frequency ratio in exact agreement with the predicted value for ThO.

From the above assigned isotopic frequencies for ν_3 and ν_1 of ThO_2 and using an apex angle of 106°, it is possible to estimate ν_2 the bending frequency. This has been done using a three term potential function, and yields the following results:

$$\nu_2(ThO_2^{16}) = 124 \text{ cm}^{-1}$$

$$K_1 = 5.11 \times 10^5 \text{ dynes/cm}$$

$$\frac{K_\delta}{\ell^2} = .067 \times 10^5 \text{ dynes/cm}$$

$$K_{12} = .44 \times 10^5 \text{ dynes/cm}$$

Again it should be pointed out that the massiveness of the central thorium atom makes this type of calculation quite insensitive. Experimentally it is known that the bending mode ν_2 lies below 180 cm^{-1} and therefore, some validity should be attached to the above calculated values.

Calculations involving a four term potential function, where an additional interaction force constant, (Frα), has been included, have also been attempted. In this case, use was also made of the frequencies involving the mixed isotopic species $ThO^{16}O^{18}$. These results indicate that the unobserved frequency, ν_2, could be 50 cm^{-1} greater than previous estimates.

Zirconia - The infrared spectrum of ZrO_2^{16} was also given in a previous annual report[4]. A typical spectrum of this material has been included in Figure 9 (Spectrum I). It is evident from the spectra that the situation with regard to this molecule appears to be more complicated then the

previously discussed ThO_2 study. Apparently the strong feature at 818.7 cm^{-1} becomes a triplet (780.9, 793.6 and 818.7) when a mixture of ZrO_2^{18} and ZrO_2^{16} is isolated (Spectrum II). Previously this feature had been assigned to the asymmetric stretching frequency, ν_3 of ZrO_2 and this interpretation is consistent with this isotopic study. However, it appears that the apex angle which had previously been assumed to be 180°, is found to be from the isotopic shifts, around 108°. This conclusion is further borne out by the isotopic shifts obtained from the Zr^{90}/Zr^{94} study (Spectrum III) where the doublet corresponding to ν_3 of $Zr^{94}O_2$ and $Zr^{90}O_2$ namely, 814.3 cm^{-1} and 817.7 cm^{-1}, was used to obtain an angle around 110°. This doublet separation also rules out the remote possibility that these features are due to a molecule such as Zr_2O_2 rather than ZrO_2 since the shift ($\sim$ 3.4 cm^{-1}) is too large to be due to a molecule such as Zr_2O_2. The shift from the O^{18}/O^{16} spectrum does not allow an unambiguous exclusion of this molecule from consideration. It would appear then at first glance, since the geometry of ZrO_2 is quite similar to that of ThO_2, that the spectra of these two molecules should be quite similar.

Indeed the triplet 839 cm^{-1}, 869 cm^{-1} and 884 cm^{-1} (Spectrum II) obtained from the O^{18}/O^{16} study could be a likely candidate for ν_1, the symmetric stretch. However, when the rest of the spectra are examined this conclusion becomes less certain. In the previous annual report[4], it was suggested that the features at 960 cm^{-1} and 910 cm^{-1} (958.6 cm^{-1} and 908.7 cm^{-1} for the grating) were in fact due to ZrO and that 960 cm^{-1} was due to ground state ZrO and that 910 cm^{-1} was due to a frozen in electronically excited state. This assignment is fully collaborated by both of the isotopic studies. In the O^{18}/O^{16} spectrum, 960 cm^{-1} and 948 cm^{-1} are isotopic pair and 910 cm^{-1} and 869 cm^{-1} form the other isotopic pair. While in the Zr^{94}/Zr^{90} study 958.6 cm^{-1} and 955.7 cm^{-1} form one pair and 908.7 cm^{-1} and 905.9 cm^{-1} form the other pair. In both cases the observed frequency ratios for each pair are in excellent agreement with the predicted values for the molecule ZrO. The above reasoning can even be extended to the O^{16} - O^{18} pair at 884 cm^{-1} and 839 cm^{-1} and indeed here again the frequency ratio agrees with that of ZrO. Unfortunately, the intensities of the spectral features of the Zr^{94}/Zr^{90} study were extremely weak and

therefore no splitting could be resolved in the case of the band shown at 882 cm^{-1} (this would correspond to the band at 884 cm^{-1} in the other spectra). The appearance of the band at 882 cm^{-1} does indeed indicate that it consists of more than one component. It would then seem likely that the band at 884 cm^{-1} can also be assigned to a frozen in excited state of ZrO. The possibility of maintaining in the matrix an electronically excited state is certainly an intriguing one and should be investigated further. In the case of ZrO, singlet, triplet and quintuplet states are possible and any radiative transitions between these states of different multiplicity are forbidden. It is conceivable that the matrix could maintain these different excited states which were thermally populated during the vaporization process even though, at matrix temperatures, only the ground state should be populated. There appears to be some evidence for the existence of several low lying electronic states in ZrO, and therefore, these states could become fairly populated at vaporization temperatures. The short wavelength features at 1310 cm^{-1}, 1835 cm^{-1} and 1855 cm^{-1} do not appear to be related to the vibrational spectra of either ZrO_2 or ZrO and

may possibly be due to impurities or indeed to several low lying electronic states of these molecules.

It is seen from the above discussion that there is some doubt as to the assignment of ν_1 of ZrO_2 since the features of the spectrum which could be ascribed to it namely, 839 cm^{-1}, 869 cm^{-1} and 884 cm^{-1} could equally well be ascribed to ZrO. Unfortunately, the intensities of the spectral bands obtained in both isotopic studies were such that no reliable estimates of their relative strengths could be made so that an assignment on this basis is not possible. It is conceivable that a coincidence occurs at the 869 cm^{-1} frequency in the O^{18}/O^{16} study. This would then allow a consistent assignment to be made since both the 910 cm^{-1} feature for ZrO and the 884 cm^{-1} feature for ZrO_2 would have their proper isotopic counterparts (i.e., 910 cm^{-1} and 869 cm^{-1}, 884 cm^{-1}, 869 cm^{-1} and 839 cm^{-1}). Until a more intense spectrum is obtained on the isotopically enriched materials, no resolution of this problem can be made. Experimentally it appears to be quite difficult to obtain more intense spectra since we are already working near the upper temperature limit of the apparatus and also because the spectrum

obtained at higher temperatures appear to be complicated by spurious features[4]. As has already been mentioned, the geometry of ZrO_2 is similar to ThO_2. An estimate of both ν_1 and ν_2 can be made by scaling the ThO_2 force constants through the observed frequency, ν_3. This procedure resulted in estimates for ν_1 and ν_2 equal to $\sim$845 cm^{-1} and $\sim$137 cm^{-1} respectively. Although admittedly approximate, this calculation adds some credence to the assignment of ν_1 to the observed frequency 884 cm^{-1} (for ZrO_2^{16}).

III. RESONANCE LINE ABSORPTION STUDIES

A. Background and Introduction

The technique of resonance line absorption as applied to the measurement of the vapor pressure of atomic constituents over high temperature materials has been described in detail in the previous annual reports[1,2,3,4]. Basically, the technique consists of heating the material of interest in a cell of known dimensions. This cell is placed at the center of a graphite tube furnace where temperatures as high as 3000°K can be maintained. The furnace is filled with an inert gas to minimize diffusion out of the cell and the resonance line absorption of the hot atomic vapors is photometrically

measured. Two different techniques have been developed here for following this absorption. The first consists of using as a source an extremely narrow resonance line of the atom to be measured. This line is produced in a special liquid nitrogen cooled hollow cathode. The hollow cathode light then passes through the cell and the absorption is measured with a spectrophotometer. Since the source is extremely narrow, the absorption of this light takes place at the center of the wider absorption line of the hot atoms in the furnace, and therefore, the absorption can be simple related to the density of these atoms from the known oscillator strength of the resonance transition. The technique has shown extreme sensitivity to small concentrations of atoms. Pressures as low as 10^{-8} to 10^{-9} atm. have been measured. Generally, reliable oscillator strengths are not available and, therefore, the technique has been used to obtain the vapor pressure of a particular atom relative to the vapor pressure over the pure metal. Such measurements lead directly to the determination of the free energy of formation of the material in question. The second technique makes use of a continuous source rather than the hollow cathode. Absorption

of the continuum by the hot furnace atoms is measured and the total absorption (absorption vs. wavelength) is determined by scanning through the line. From these measurements, the total absorption vs. relative concentration (curve of growth) can be determined for the pure metals and, consequently, the relative concentration (activity) of the particular atomic species over the refractory material can be obtained. This again leads directly to the free energy of formation of the refractory material.

Although the total absorption technique is generally less sensitive and more time consuming than the hollow cathode technique, it can be used over a much larger pressure range and hence can be used in conjunction with the Second Law to obtain heats of formation. Generally the hollow cathode results must be used only with the Third Law since it is usually confined to a limited pressure and hence temperature range.

During this past year's investigations the second technique has been applied to the measurement of the partial pressure of boron over HfB_2 while the first technique was applied to the measurement of the partial pressures of

titanium and zirconium over TiN and ZrN respectively.

B. Experimental

The basic techniques have been adequately described elsewhere[2,3,4]. In the ZrN study it was necessary to isolate the sample cell from the carbon environment of the furnace in order to prevent the formation of the corresponding carbide. Apparently the temperatures in this study were sufficiently high so that the vapor pressure of the grap' ' ' was great enough to produce the carbide. In the case of the measurements made on TiN and the pure metals, the temperature was low enough so that the vapor pressure of carbon was no problem. A schematic of the general absorption cell set-up is given in Figure 10. The tantalum liner was used in those determinations, as indicated above.

Hafnium Diboride - A sample of zone refined HfB_2 wa- obtained from the Arthur D. Litt Company having the following analysis:

Sample Lot # - 302-2

B - 10.6 - 10.7%

Nb - .52%

Ta - .10%

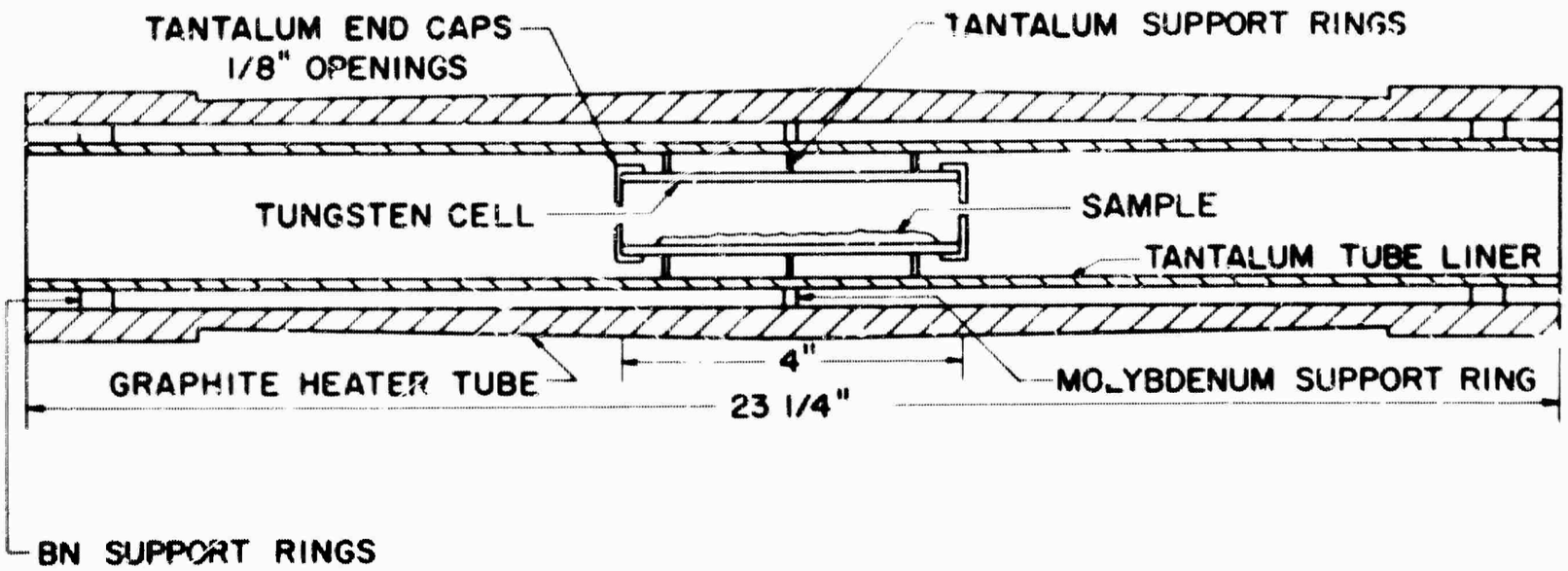

Figure 10. Absorption Cell Apparatus

Ti - .25%

H - 3.36 P.P.M.

N - 101 P.P.M.

O - 16 P.P.M.

C - 1300 P.P.M.

By mixing this material with an equimolar amount of spectroscopic grade graphite, the following univariant reaction was followed by measuring the total absorption of the two boron resonance lines:

$$HfB_2(s) + C(s) = HfC(c) + 2\ B(g) \qquad (2)$$

The equilibrium constant for (2) is completely determined by the vapor pressure of boron. Total absorption measurement of the boron 2497 Å and 2496 Å resonance lines were carried out at various temperatures using an inert gas atmosphere of helium such that the "a" value was the same as that of the pure boron determinations. From the total absorption measurements, the corresponding pressures of boron were determined via the curve of growth. These results are summarized in Table III.

Titanium Nitride - The method used in this study is entirely analogous to that used in the measurement of the

TABLE III

VAPOR PRESSURE OF BORON OVER $HfB_2(s) + C(s)$

Temperature °K	1/T x 10^5	Ag $(\ln 2)^{1/2}/\pi\Delta\nu_D$		Log P Boron	
		λ- 2497 Å	λ- 2496 Å	λ- 2497	λ- 2496
2268	44.09	1.07	0.65	-6.15	-6.15
2276	43.94	1.13	0.70	-6.10	-6.10
2294	43.59	1.26	0.85	-6.02	-5.99
2303	43.42	1.36	0.92	-5.95	-5.94
2326	42.99	1.61	1.11	-5.79	-5.80
2345	42.64	1.74	1.29	-5.69	-5.68
2357	42.43	1.78	1.39	-5.66	-5.62
2367	42.28	1.93	1.44	-5.56	-5.58
2385	41.93	2.06	1.55	-5.48	-5.51
2406	41.56	2.27	1.79	-5.36	-5.34

vapor pressure of titanium over TiB_2[4] and TiC[3]. The reaction followed is given by (3):

$$TiN(s) = Ti(g) + \tfrac{1}{2} N_2(g) \qquad (3)$$

The titanium partial pressures at fixed nitrogen pressures were determined using the hollow cathode technique.

It should be pointed out that the resonance line absorption technique offers a distinct advantage over mass spectrometric and Knudsen effusion techniques in the case of TiN, since ambient pressures of nitrogen can be easily maintained and measured in the system without hindering the spectroscopic measurements. Furthermore, the vapor pressure of titanium can be measured as a function of the nitrogen pressure allowing the equilibrium constant for the vaporization to be obtained.

A sample of TiN was obtained from the Metal Hydrides Company. This material had a nominal composition of $TiN_{.834}$, however, after long heating in pure nitrogen at around 1800°C, the composition was found to be $TiN_{.991}$. This TiN was then loaded into a 4" long tungsten cell, 1/2" in diameter, with 1/32" wall. Tantalum end caps having 1/4" openings were fitted to this cell and the cell with TiN was

placed in the center of the hot zone of the carbon resistance furnace. The 3371 Å resonance line was generated in a hollow cathode discharge tube cooled to liquid nitrogen temperatures. The absorption of this line was measured at various nitrogen pressures in the furnace; the pressures being read on a mercury manometer. Corresponding absorption measurements were made over pure titanium metal, however, in this case, argon was used in the furnace instead of nitrogen under conditions such that the pressure broadening parameters were the same as in the TiN measurements. From a comparison of the absorption of the Ti 3371 Å line over TiN and titanium metal, the partial pressures of titanium over TiN could be obtained. The results of these measurements are given in Table IV.

Zirconium Nitride - In a manner completely analogous to the TiN work and to the ZrC[3] and ZrB_2[4] studies, the vapor pressure of zirconium over ZrN at various partial pressures of nitrogen were determined using the hollow cathode technique.

A sample of ZrN was obtained from the Metal Hydrides Company and was heated in pure nitrogen at around 1800°C to ensure complete conversion to the nitride. The sample was

TABLE IV

EXPERIMENTAL RESULTS FOR THE ABSORPTION OF

Ti 3371 Å LINE OVER TiN(s) AND Ti(s)

Material	Temperature °K	$P_{ambient}$ cm hg	I/I_o	$AP = T^{3/2} \times 10^{-4}$	$\log I_o/I$	P_{Ti} Atm.
	2119	33.5	.775	1.079		2.76×10^{-8}
	2119	33.6	.774	1.085		2.78×10^{-8}
	2119	33.4	.771	1.102		2.82×10^{-8}
TiN(s)	2120	25.5	.720	1.393		3.36×10^{-8}
	2119	25.5	.734	1.309		3.16×10^{-8}
	2119	25.5	.719	1.398		3.37×10^{-8}
	2119	15.4	.674	1.672		3.90×10^{-8}
	2121	15.4	.661	1.756		4.09×10^{-8}
	2119	5.0	.484	3.074		6.67×10^{-8}
	2120	5.0	.491	3.016		6.55×10^{-8}
	2141	5.0	.369	4.289		9.31×10^{-8}
	2140	5.0	.369	4.286		9.31×10^{-8}
	2088	5.0	.731	1.298		2.82×10^{-8}
	2088	5.0	.745	1.219		2.65×10^{-8}
	2089	5.0	.730	1.305		2.83×10^{-8}
	1632	29.3	.730	.902		
	1631	29.3	.743	.850		
	1632	29.3	.732	.893		
	1632	22.4	.724	.924		
	1631	22.4	.723	.928		
	1631	22.4	.717	.952		
	1632	13.5	.716	.957		
Ti(s)	1632	13.5	.705	1.000		
	1632	13.5	.719	.945		
	1632	4.4	.694	1.046		
	1632	4.4	.700	1.022		

P titanium metal at 1632°K = 2.254×10^{-8} (JANAF Tables)

placed in a cell completely similar to the TiN study except that a tantalum liner was used (Figure 10) to isolate the sample from the carbon environment. Measurements of the absorption of the Zr 3601 Å resonance line were made over the nitride and over the pure metal under conditions such that the pressure broadening in both cases was approximately the same. Partial pressures of zirconium at various nitrogen pressure were determined. These results appear in Table V.

C. Results and Discussion

Hafnium Diboride - The vapor pressure data presented in Table III was subjected to both a Second and Third Law treatment. The heat of reaction (2) namely:

$$HfB_2(s) + C(s) = HfC(s) + 2\ B(g) \qquad (2)$$

obtained by these two methods are as follows:

$$\Delta H^o_{298}(2)\ \text{(Second Law)} = 290.2\ \text{kcal/mole}$$

$$\Delta H^o_{298}(2)\ \text{(Third Law)} = 288.2\ \text{kcal/mole}$$

The agreement between these values appears to be satisfactory and indicates that the data are self consistent. These results are also presented in Figure 11 and Table VI. In order to obtain the heat of formation of HfB_2 from the heat of reaction (2), it is necessary to know the heat of formation

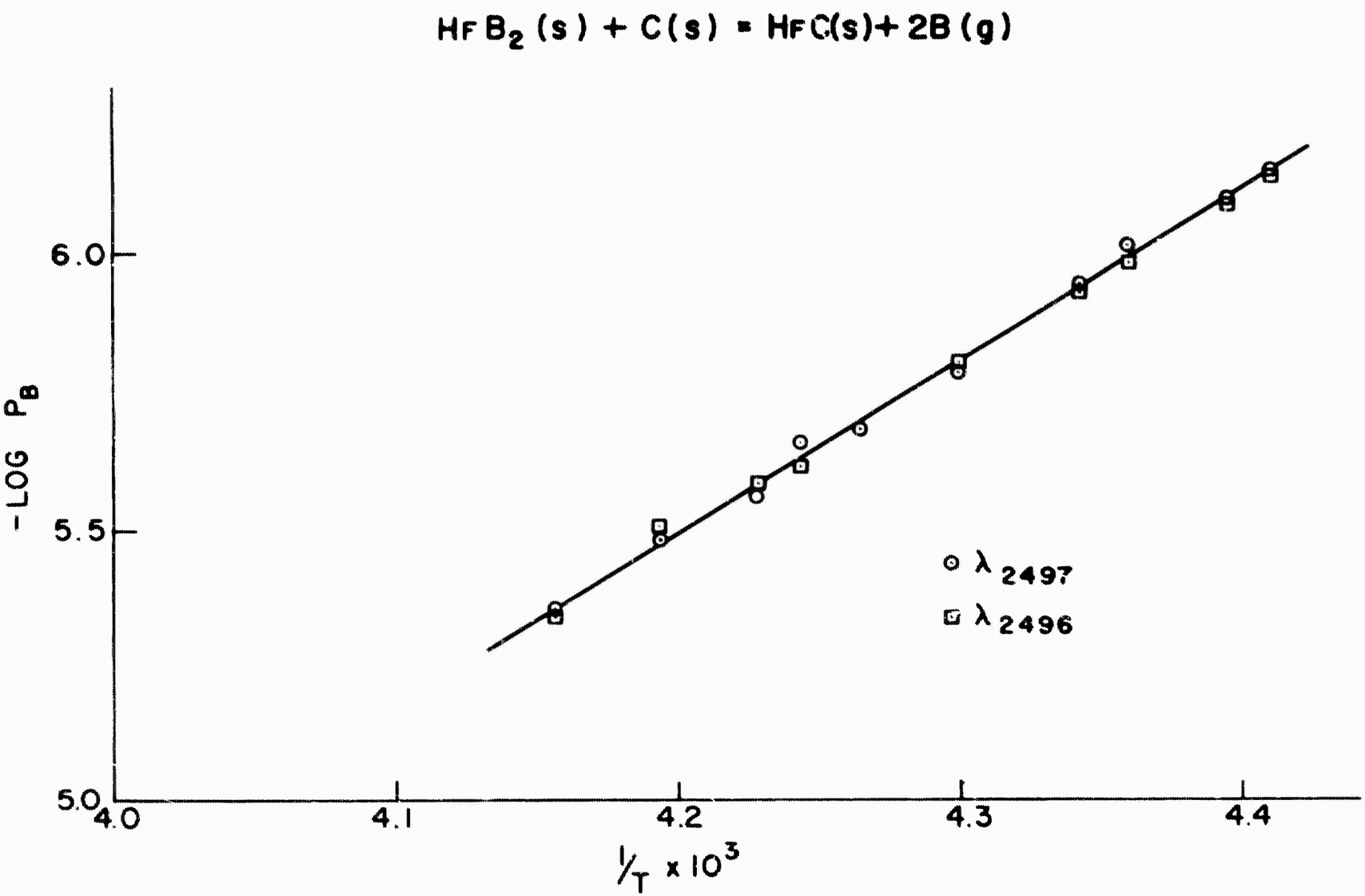

Figure 11. Log P_B vs 1/T - HfB_2

TABLE V

EXPERIMENTAL RESULTS FOR THE ABSORPTION OF

Zr 3601 Å LINE OVER ZrN(s) AND Zr(s)

Material	Temperature ^{o}K	$P_{ambient}$ cm hg	I/I_o	$AP = T^{3/2} \log I_o/I \times 10^{-4}$	Zr Atm.
	2523	20.0	.718	1.698	3.65×10^{-8}
Run #1	2523	20.0	.745	1.614	3.48×10^{-8}
	2522	20.0	.740	1.655	3.56×10^{-8}
	2522	20.0	.746	1.610	3.46×10^{-8}
	2520	20.0	.760	1.504	3.23×10^{-8}
	2521	30.0	.803	1.205	2.67×10^{-8}
ZrN(s)	2522	30.0	.803	1.205	2.67×10^{-8}
	2521	10.0	.607	2.743	5.43×10^{-8}
	2523	20.0	.750	1.582	3.40×10^{-8}
Run #2	2521	20.0	.736	1.682	3.62×10^{-8}
	2521	10.0	.612	2.700	5.35×10^{-8}
	2524	10.0	.570	3.094	6.13×10^{-8}
	2523	10.0	.600	2.813	5.57×10^{-8}
	2521	10.0	.585	2.946	5.84×10^{-8}
	2098	18.0	.882	.5241	P Zirconium metal at $2100^{o}K = 1.146 \times 10^{-8}$ (JANAF tables)
	2099	18.0	.881	.529	
	2100	18.0	.883	.520	
Zr(s)	2100	9.0	.868	.592	
	2100	9.0	.869	.587	

TABLE VI

HEAT OF REACTION FOR

$HfB_2(s) + C(s) = HfC(s) + 2B(g)$ (2)

Temperature °K	-fef	$\frac{\Delta F^\circ}{T}$(2497A)	$\frac{\Delta F^\circ}{T}$(2496)	$H^\circ_{298}(1)$ kcal/mole 2497A	$H^\circ_{298}(1)$ kcal/mole 2496A
2268	70.806	56.304	56.267	288.29	288.20
2276	70.801	55.837	55.782	288.23	288.10
2294	70.789	55.096	54.785	288.78	288.07
2303	70.781	54.473	54.345	288.46	288.17
2326	70.766	52.954	53.110	287.77	288.14
2345	70.752	52.066	51.993	288.01	287.84
2357	70.743	51.828	51.407	288.90	287.91
2367	70.738	50.886	51.096	288.88	288.38
2385	70.727	50.172	50.401	288.34	288.89
2406	70.709	49.028	48.891	288.09	287.76

ΔH°_{298} Ave. = 288.2 kcal/mole

of HfC. We have chosen to use the value suggested by Schick, et.al.[15], namely -55.0 kcal/mole. The resulting heat of formation of HfB_2 is:

$$\Delta H^{o}_{298} \text{ (Second Law)} = -79.9 \text{ kcal/mole}$$

$$\Delta H^{o}_{298} \text{ (Third Law)} = -78.0 \text{ kcal/mole}$$

It should be pointed out that the heat of formation obtained is independent of the heat of vaporization of boron (but not the listed vapor pressures) since the curve of growth was calculated relative to pure boron. These values for $\Delta H^{f}HfB_2$ are quite consistent with other values[15].

Titanium Nitride - From the results given in Table IV, the corresponding equilibrium constants for the reaction:

$$TiN(s) = Ti(g) + \tfrac{1}{2} N_2(g) \qquad (3)$$

can be calculated. By imposing the Third Law and by using the free energy functions for TiN(s), Ti(g) and $N_2(g)$ as given in the JANAF tables, the heat of reaction (3) at 298°K was found to be 193.88 $\pm$ .44 kcal/mole. The error given here is only representative of the scatter about the mean value and does not include any errors associated with the free energy functions. These results are given in Table VII for the data at 2120°K. The heat of formation of TiN(s) can

TABLE VII

HEAT OF VAPORIZATION OF TiN(s)

$TiN(s) = Ti(g) + \frac{1}{2} N_2(g)$ (3)

Temperature °K	$P_{Nitrogen}$ atm	$P_{Titanium}$ atm x 10^8	K_P x 10^8	Δfef	ΔH^o_{298} kcal/mole(1)
2119	.441	2.76	1.83	56.0845	193.86
2119	.442	2.78	1.85	56.0845	193.83
2119	.439	2.82	1.87	56.0845	193.78
2120	.335	3.36	1.95	56.0835	193.70
2119	.335	3.16	1.83	56.0845	193.87
2119	.335	3.37	1.95	56.0845	193.70
2119	.203	3.90	1.76	56.0845	194.05
2121	.203	4.09	1.84	56.0820	194.02
2119	.066	6.67	1.72	56.0845	194.13
2120	.066	6.55	1.69	56.0835	193.80

$\Delta H^o_{298\ ave.} = 193.88 \pm .44$

be obtained from this heat of vaporization by using the known heat of formation for Ti(g). The JANAF value of 112.49 kcal/mole was used which leads to a value of -81.39 kcal/mole for the heat of formation of TiN(s). This value is in excellent agreement with the value -80.5 $\pm$ 1.5 kcal/mole given by JANAF.

Zirconium Nitride - In a completely analogous fashion the data of Table V was subjected to a Third Law analysis. Again the free energy functions for the components of the reaction:

$$ZrN(s) = Zr(g) + \tfrac{1}{2} N_2(g) \qquad (4)$$

were taken from the JANAF tables. The heat of this reaction at 298^{o}K was found to be 227.6 $\pm$ .3 kcal/mole. The error shown again only reflects the scatter from the mean value. These results are presented in Table VIII.

By using the value for the heat of formation of Zr(g) as given by JANAF, i.e., 145.42 kcal/mole, the heat of formation of ZrN(s) at 298^{o}K is found to be -82.8 kcal/mole. This value differs from the JANAF accepted value by about 4.5 kcal/mole. On the other hand it is in excellent agreement with the value obtained by Hoch, et.al[17] namely -81 kcal/mole.

TABLE VIII

HEAT OF VAPORIZATION OF ZrN(s)

$ZrN(s) = Zr(g) + \frac{1}{2} N_2(g)$ (4)

Temperature ^oK	P_{N_2} atm.	$P_{Zr} \times 10^8$ atm.	$K_p \times 10^8$	-fef	$\frac{\Delta F^o}{T}$	$\Delta H^o_{298(s)}$ kcal/mole
2523	.263	3.65	1.87	54.8575	35.365	277.63
2523	.263	3.48	1.78	54.8575	35.463	227.88
2522	.263	3.56	1.82	54.8595	35.418	227.68
2522	.263	3.46	1.77	54.8595	35.474	227.82
2520	.263	3.23	1.66	54.8605	35.601	227.96
2521	.395	2.67	1.67	54.8610	35.589	228.02
2522	.395	2.67	1.67	54.8596	35.589	228.11
2521	.132	5.43	1.97	54.8610	35.261	227.20
2523	.263	3.40	1.74	54.8575	35.508	227.99
2521	.263	3.62	1.85	54.8610	35.386	227.51
2521	.132	5.35	1.94	54.861	35.291	227.27
2524	.132	6.13	2.22	54.8540	35.023	226.85
2523	.132	5.57	2.02	54.8575	35.211	227.24
2521	.132	5.84	2.12	54.8575	35.115	226.82

ΔH^o_{298} Ave. = 227.6 $\pm$ .3

IV. REFERENCES

1. Coffman, J. A., et.al, WADD T.R. 60-646, Part I (February 1961).

2. Ibid. Part II (January 1963).

3. Kibler, G. M., et.al., WADD T.R. 60-646, Part III, Vol. 2, (March 1964).

4. Ibid. Part IV (January 1964).

5. Linevsky, M. J., J. Chem. Phys. 34, 587 (1961).

6. Sommer, White, Linevsky and Mann, J. Chem. Phys. 38, 87 (1963).

7. White, Seshadri, Dever, Mann and Linevsky, J. Chem. Phys. 39, 2463 (1963).

8. Linevsky, White and Mann, J. Chem. Phys. 41, 542 (1964).

9. Linevsky, M. J., J. Chem. Phys. 38, 658 (1963).

10. Brewer, L., Somayajulu, R. S. and Brackett, E., Chem. Rev. 63, 111 (1963).

11. N.B.S. Report #6928 "Preliminary Report on the Thermodynamic Properties of Selected Light Element Compounds," July 1960.

12. Herzberg, G., "Infrared and Raman Spectra," D. Van Nostrand Co. (1945).

13. Farber, M. and Peterson, H. L., Trans. Faraday Soc. 59, 836 (1963).

14. D. E. Mann, Private Communication, Washington D. C., (1964).

15. Schick, H. L., et.al., Fourth Quarterly Progress Report, "Thermodynamics of Certain Refractory Compounds," Part II, Research and Development Division, AVCO Corporation, June 1963.